SCIENTIFIC REPORTS

OPEN

SUBJECT AREAS:
APPLIED MICROBIOLOGY
ASSAY SYSTEMS

Received
8 April 2014

Accepted
17 June 2014

Published
9 July 2014

Correspondence and requests for materials should be addressed to J.R.M. (janroelof.vandermeer@unil.ch)

Escherichia coli ribose binding protein based bioreporters revisited

Artur Reimer[1], Sharon Yagur-Kroll[2], Shimshon Belkin[2], Shantanu Roy[1] & Jan Roelof van der Meer[1]

[1]Department of Fundamental Microbiology, University of Lausanne, Bâtiment Biophore, Quartier UNIL-Sorge 1015 Lausanne, Switzerland, [2]Department of Plant and Environmental Sciences, The Alexander Silberman Institute of Life Sciences, The Hebrew University of Jerusalem, Jerusalem 91904, Israel.

Bioreporter bacteria, i.e., strains engineered to respond to chemical exposure by production of reporter proteins, have attracted wide interest because of their potential to offer cheap and simple alternative analytics for specified compounds or conditions. Bioreporter construction has mostly exploited the natural variation of sensory proteins, but it has been proposed that computational design of new substrate binding properties could lead to completely novel detection specificities at very low affinities. Here we reconstruct a bioreporter system based on the native *Escherichia coli* ribose binding protein RbsB and one of its computationally designed variants, reported to be capable of binding 2,4,6-trinitrotoluene (TNT). Our results show *in vivo* reporter induction at 50 nM ribose, and a 125 nM affinity constant for *in vitro* ribose binding to RbsB. In contrast, the purified published TNT-binding variant did not bind TNT nor did TNT cause induction of the *E. coli* reporter system.

Construction of bioreporter bacteria typically starts with identifying a sensory protein that controls expression of a target gene promoter in dependence on one or more chemical inducers[1–8]. As an example, the ArsR protein represses its cognate promoter P_{ars}, but when cells are exposed to arsenite (AsIII), this oxyanion will interact with ArsR causing it to lose affinity for the operator site close to P_{ars}, thus increasing the rate of transcription from P_{ars}[6]. The expression of reporter genes, such as those for luciferase, autofluorescent proteins or beta-galactosidase, when coupled to P_{ars}, will consequently increase in the presence of arsenite; it is this increase in reporter protein signal or activity that is quantified in the bioreporter assay[9]. Despite the interest in and potential applicability of bioreporter assays, the weak part in their design is the availability of suitable sensory proteins for recognition of the target chemicals. Most of the "low-hanging fruits" in form of bacterial transcription regulators for e.g., heavy metals and metalloids, organic compounds or global stress responses, have been exploited[7,10–14]. Although it has been shown to be possible to somewhat expand substrate recognition properties of known transcription regulators through mutagenesis and selection, this is a rather cumbersome approach[15–20]. In this context, a landmark study over ten years ago suggested a completely different framework for the construction of bioreporter systems, based on computerized design of *de novo* substrate binding properties of periplasmic binding proteins (PBPs)[8]. Substrate binding to the redesigned PBP would lead to an interaction with a hybrid membrane receptor, thereby triggering reporter gene expression, as will be explained more in detail below (Fig. 1).

PBPs consist of a broad class of proteins that carry a conserved protein structure, the bilobal structural fold[21]. PBPs scavenge molecules for the cell, which they can present to specific transporter channels, and/or link compound binding to chemotactic movement. As an example, the galactose- (GBP) and ribose-binding proteins (RBP) of *Escherichia coli* enable the cell to sense galactose and ribose, respectively[22]. The sugars are bound by their respective PBP, and a fraction of sugar-bound GBP and RBP binds to the Trg chemoreceptor; the other fraction is presented to the transport channels MglAC (for GBP-galactose) or RbsAC (for RBP-ribose)[23].

The binding of the PBP to a chemoreceptor can be transformed into *de novo* gene expression by using a hybrid membrane chemoreceptor-histidine kinase. This was shown almost 20 years ago by the group of Hazelbauer, who linked the EnvZ histidine kinase of the *E. coli* osmoregulation system to the Trg receptor via the so-called HAMP domain (Fig. 1a)[24]. The HAMP domain is a conserved domain among *h*istidine kinases, *a*denylyl cyclases, *m*ethyl-accepting chemotaxis proteins and *p*hosphatases, and plays a crucial role in signal transduction[25]. The resulting hybrid receptor kinase (named TrzI) combines the 265 N-terminal amino acids of Trg with the 230 C-terminal amino acids of EnvZ[24]. Galactose-GBP and/or ribose-RBP binding to TrzI will trigger histidine kinase activity of the cytoplasmic EnvZ-domain, leading to phosphorylation of the cognate DNA-binding response regulator OmpR. Phosphorylated OmpR (OmpR ~ P) binds the low affinity sites within the OmpC promoter (P_{ompC}) and increases transcription rate from this promoter (Fig. 1a)[26]. A proof of concept was presented by

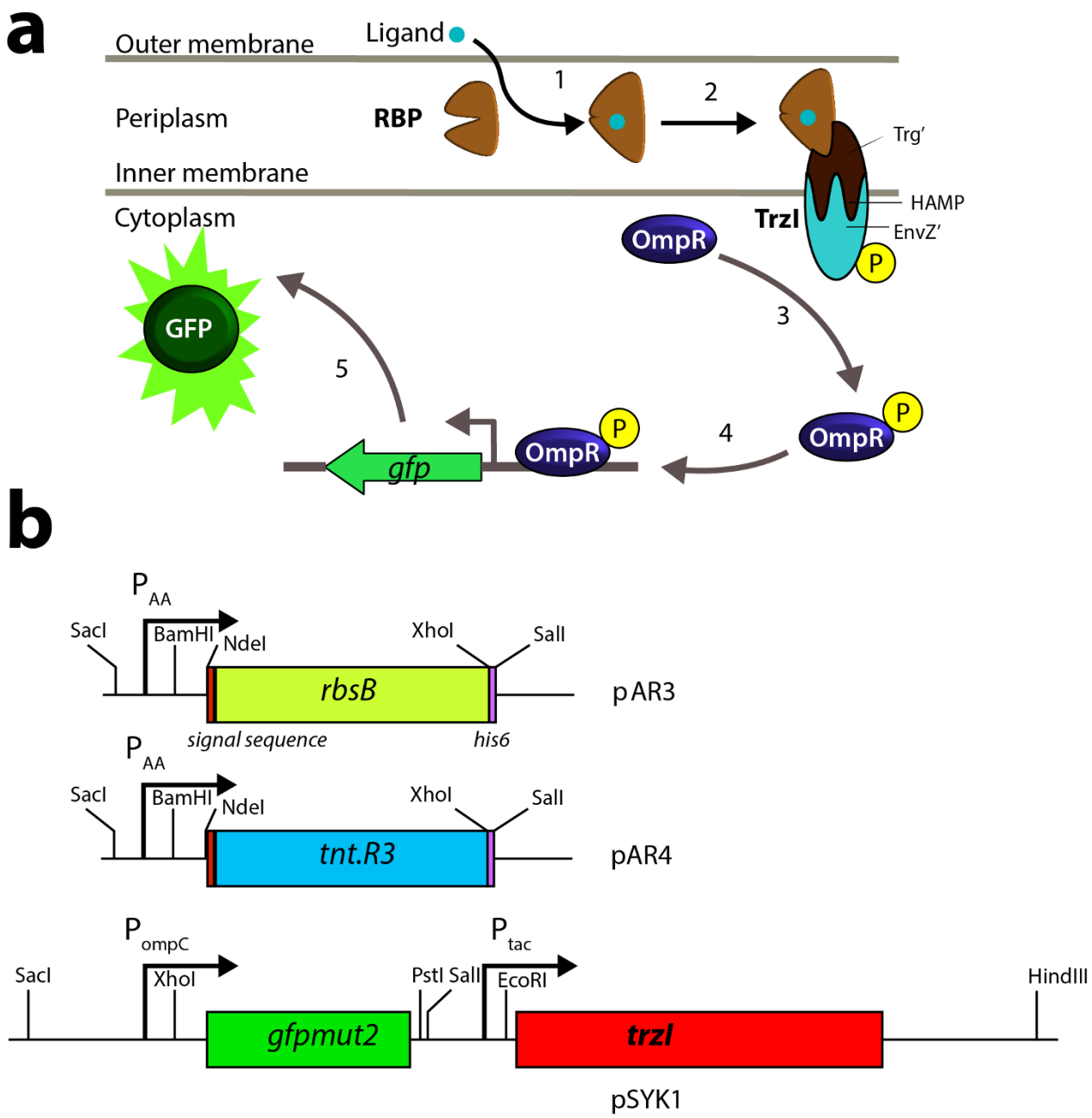

Figure 1 | Schematic outline of the ribose-binding protein based reporter signaling chain. (a) Ribose-binding protein (RBP) captures its ligand, leading to a conformational change. Ribose-RBP binds the TrzI hybrid transmembrane receptor, which causes a phosphorylation cascade leading to OmpR ~ P binding the *ompC*-promoter and consecutive *gfpmut2* expression. (b) Relevant plasmid constructions. *rbsB* or *tnt.R3* with original *rbsB* periplasmic export signal sequence and 3′-hexahistidine tag under transcriptional control of the weak constitutive P_{AA} promoter[29]. Plasmid pSYK1 with *gfpmut2* under the *ompC* promoter control and *trzI* under control of P_{tac} (note that pSYK1 carries the $lacI^q$ gene).

fusing P_{ompC} with the gene coding for β-galactosidase (*lacZ*) in *E. coli*, demonstrating that *trzI* expression yielded enhanced β-galactosidase activity when exposed to increasing ribose concentrations[24].

A major conceptual advancement was made when it was proposed that by molecular dynamics modeling, on the basis of the resolved crystal structure of RBP, with and without ligand, it would be possible to predict the amino acid changes in RBP necessary for binding with new ligands[27]. This would create a possibly universal scaffold for engineering of new ligand-binding specificities, which could all be hosted in the same signaling "chassis" presented by the hybrid TrzI-OmpR system. To provide proof of principle, the binding pockets of glucose-binding protein (GBP), ribose-binding protein (RBP), arabinose-binding protein (ABP), glutamine-binding protein (QBP) and histidine-binding protein (HBP) were redesigned by computational simulation in order to bind toxic and non-natural molecules, such as serotonin, dinitrotoluene and TNT[8]. Simulation results suggested that nM binding affinities could be obtained, and experimental data were presented showing that expressing the mutant RBPs in an *E. coli* TrzI-OmpR background with *ompCp-lacZ* reporter led to nM detection specificity of TNT by measuring β-galactosidase activity[8].

Motivated by the potential importance and implications of a universal scaffold for the engineering of bioreporter ligand specificity, we have set out to repeat the construction of one of the developed bioreporter strains with reported nM affinity for recognition of TNT[8]. A wide variety of methods is available for detection of TNT

(see, for example, ref. 28), but bioreporter-based assays could be interesting for field application. Genes for both wild-type (*rbsB*) and mutant RBP (*tnt.R3*) were produced by DNA synthesis and cloned in an *E. coli* TrzI-OmpR background expressing the GFPmut2 protein from the *ompC*-promoter, to measure sensitivity of the reporter strains for ribose and TNT, respectively. We examined expression of wild-type and mutant proteins in the reporter strains, and have investigated ligand binding of the purified proteins by iso-thermal calorimetry (ITC). Whereas wild-type RBP produced an excellent and sensitive ribose sensor in *E. coli*, the published TNT-binding RBP variant did not show any significant binding to TNT, and the bioreporter cells harbouring it did not display any response to TNT or ribose.

Results

In vitro characterization of RbsB and TNT.R3 substrate binding. To test substrate binding by RbsB and TNT.R3 we purified both proteins from *E. coli* and determined the heat released by substrate addition to the purified protein fractions by isothermal microcalorimetry (ITC). Both proteins were overexpressed from the T7 promoter as C-terminal hexahistidine tagged variants in *E. coli* BL21 (DE3) pLysS using IPTG induction of the T7 RNA polymerase. Proteins were purified from culture-cleared lysates using Ni-NTA affinity chromatography. Figure 2 shows the different affinity binding steps and the purity of the final protein fraction (Elution II, at 250 mM imidazol). Concentrations of RbsB-His_6 and TNT.R3-His_6 after elution were between 0.2 and 0.8 mg/mL (Table 1).

Addition of 250 μM ribose to 34 μM RbsB-His_6 solution produced clear evidence for ribose binding with successively decreased heat release upon accumulated ribose additions (Fig. 3a). Assuming a single binding site for ribose per RbsB, an affinity constant (K_d) of 125 nM was calculated from the fitted data sets. Titration of buffer into RbsB-His_6 solution, or of ribose solution into buffer produced no heat release (Figure S1). In contrast, neither 1 mM TNT nor 1 mM ribose titration into 20 μM TNT.R3-His_6 solution released heat that was different from the addition of buffer alone (Figure 3b, c). Titration of TNT alone into buffer did not produce any consistent heat release as well (Figure S1).

Because the maximum aqueous solubility of TNT, 140 mg/L at 20°C, may have been limiting for saturation of TNT.R3 binding sites, we also tested the opposite titration in ITC (i.e., protein into substrate solution). In this manner, the TNT concentration in the measurement cell can be maintained below aqueous solubility. However, titration of 50 μM TNT.R3-His_6 solution into 150 μM TNT also did not produce consistent heat release (Figure S1A, B). In contrast, titration of 100 μM RbsB-His_6 solution into 4 μM ribose did produce heat release (Figure S1C), although in comparison to the binding curve in Figure 3a the injection peaks were not as clear. This may have been due to secondary effects caused by the dissolution of protein agglomerates during the injection. We thus concluded from the *in vitro* experiments that purified RbsB-His_6 is indeed capable of binding ribose, but that TNT.R3-His_6 neither binds TNT nor ribose, although the protein can be purified and is detectable on SDS-PAGE without any apparent degradation (Fig. 2b).

RBP-based bioreporter assays. To verify that *E. coli* expressing the TrzI-hybrid-OmpR signaling chain is indeed a good chassis for an RbsB-based bioreporter, we reconstructed a reporter strain using *gfpmut2* instead of the original *lacZ* under control of the *ompC* promoter (Fig. 1b, plasmid pSYK1), and measured induction of GFPmut2 over time in the presence of different sugars. This *E. coli* (strain 4175) lacks the chromosomal *rbsB* but constitutively expresses *rbsB-his6* from a moderately constitutive promoter (P_{AA}, plasmid pAR3). In addition, this strain expresses *trzI* from the *lac* promoter and carries the *ompCp-gfpmut2* fusion (both on plasmid pSYK1). Background fluorescence of *E. coli* BW25113 strain 4175

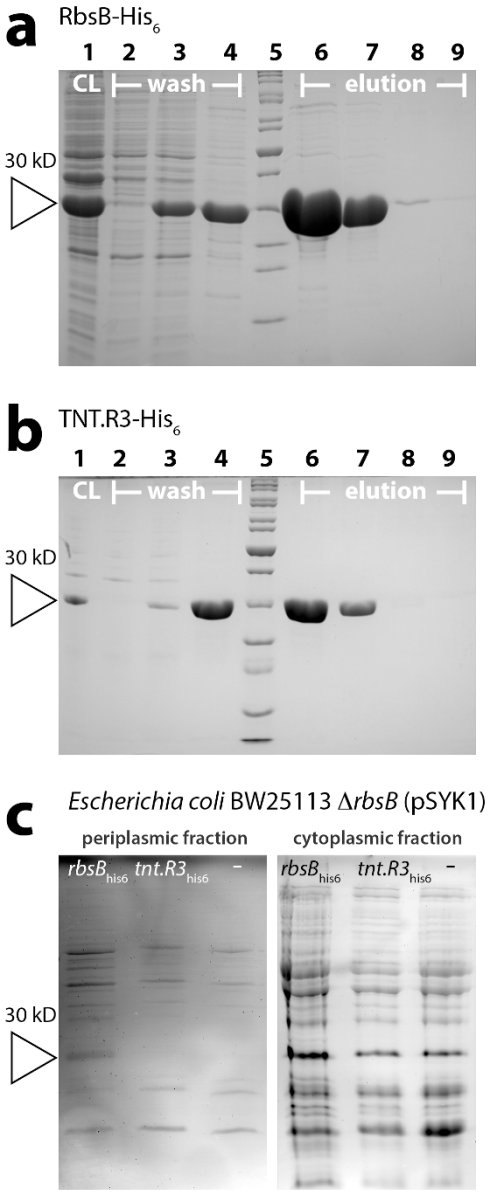

Figure 2 | Purification and expression in *E. coli* of RbsB-His_6 and TNT-His_6. (a) Coomassie-stained SDS-PAGE gel of purified fractions of RbsB-His_6 from *E. coli* BL21 (pAR1, strain 3725). Lanes: 1, cleared lysate; 2, flowthrough; 3, Washing step I; 4, Washing step II; 5, Peqgold protein marker 2; 6, Elution I; 7, Elution II; 8, Elution III; 9, Elution IV. (b) As A, but for *E. coli* BL21 (pAR2, strain 3325). Lanes: as for panel (A). (c) InVision His6-tag stained SDS-PAGE gel of cell extracts from *E. coli* BW25113 Δ*rbsB* (pSYK1) expressing *rbsB-his6* (from plasmid pAR3, strain 4175), *tnt.R3-his6* (from plasmid pAR4, strain 4176), or with empty pSTV plasmid (strain 4497). Left panel, periplasmic protein fraction. Right panel, whole soluble protein fraction. Open triangle indicates the expected position (30 kDa) of RbsB-His_6 and TNT.R3-His_6.

grown on MM with fumarate as sole carbon and energy source was very low, and the lowest measured ribose concentration that resulted in statistically significant GFPmut2 induction compared to the medium-only control within 2 h incubation time was 50 nM (Fig. 4a). Maximum induction reached 25-fold at a ribose concentration of 10 μM (Fig. 4c). To determine the reporter strain's specificity we examined GFPmut2 production upon addition of a variety of other sugars, the majority of which (xylose, arabinose, sucrose, fructose, maltose, mannose, lactose) did not elicit any GFPmut2 induction from the *E. coli* reporter strain at

Table 1 | Protein concentrations during purification of RbsB-His_6 and TNT.R3-His_6 from *E. coli* BL21 (DE3)

Sample	Total protein concentration (mg/ml)	
	RbsB-His_6	TNT.R3-His_6
Column flow through	43.9	27.1
Washing step I	22.9	14.4
Washing step II	2.4	1.2
Elution I	5.0	0.7
Elution II	0.8	0.2
Elution III	0.12	0.01

concentrations below 1 mM. In contrast, significant GFPmut2 production was observed upon incubation with galactose and glucose between 300 nM and 10 μM (Fig. 4d, e). This is likely caused by interference from GBP, which can bind either galactose or glucose, and interacts in its closed (substrate-bound) configuration with the hybrid receptor TrzI (Fig. 4f). The reaction to glucose is lower than to galactose at the same concentration, possibly due to the more rapid metabolism of this sugar.

Next, we examined the possible influence of a number of key proteins in the chemotaxis or osmolarity sensing pathways on reporter gene induction in the *trzI-ompR ompCp-gfpmut2* bioreporter strain. Figure 4b displays the characteristic GFPmut2 induction profiles of *E. coli* BW25113 carrying individual gene deletions as a function of ribose concentration, whereas Figure 4c shows the fold induction levels. In comparison to BW25113 lacking native *rbsB*, the isogenic strain with *envZ* interruption showed a loss of responsiveness to ribose (Fig. 4b). In contrast, interruption of *rbsK* increased the sensitivity of the reporter to ribose (Fig. 4b). A less drastic increase in sensitivity was obtained when deleting *trg* or *fliC*. Deleting *ompC* or *ompF* had very little effect on the sensitivity of the reporter strain for ribose (Fig. 4b).

Interestingly, depending on the host, on ribose concentration and on the deleted gene, the heterogeneity of GFPmut2 production among cells in the population varied significantly (Fig. 5). In general, the per-cell variability in GFPmut2 expression decreased at higher inducer concentrations (Fig. 5). Compared to the host without functional chromosomal *rbsB*, deletion of *fliC*, *ompC*, or *rbsK* led to a more homogenously reacting population at lower ribose concentrations (i.e., lower coefficient of variation, Fig. 5c, d, f). Conversely, deleting *ompF* or *envZ* resulted in higher cellular variability of GFPmut2 production, almost irrespective of ribose concentrations (Fig. 5a, e). Deleting the chromosomal *trg* chemoreceptor did not result in any difference of GFPmut2 heterogeneity compared to the Δ*rbsB* strain (Fig. 5b, g).

A non-functional TNT bioreporter. In contrast to the wild-type *rbsB*-based reporter, replacing *rbsB* by *tnt.R3* in an isogenic host background (*E. coli* BW25113 Δ*rbsB*, strain 4176, Table 2) led to complete loss of sensitivity to ribose (Fig. 4a). More importantly, the *tnt.R3*-based bioreporter was completely unresponsive to TNT over a broad concentration range, 0.06 to 4 μM (Fig. 4a). Since we did not observe any reporter signal from the reconstructed TNT.R3 bioreporter, but excellent sensitivity from the wild-type RbsB bioreporter for ribose, we also examined whether *E. coli* BW25113 expressed the TNT.R3 protein from the P_{AA}-promoter and periplasmic transport signal sequence at the same level as the RbsB protein (Fig. 1b). Expression of the RbsB-His_6 and TNT.R3-His_6 proteins in the BW25113 bioreporter strain is under control of the same low constitutive P_{AA}-promoter[29] in the same plasmid background. Unfortunately, anti-His_6-antibodies did not produce sufficient sensitivity and selectivity to detect both proteins in Western blots of cytoplasmic cell extracts from the BW25113 strains (not shown). In-gel staining of the His_6-tag revealed fluorescent bands with an apparent size of around 30 kDa in the cytoplasmic protein fraction, which were not completely specific for the expressed RbsB-His_6 and TNT.R3-His_6 in extracts from *E. coli* BW25113 (Fig. 2c). Analysis of the periplasmic fraction indicated presence of a detectable RbsB-His_6 but not TNT.R3-His_6 (Fig. 2c). Gel-extracted and trypsin-digested protein fractions in the size range of 28–36 kDa were further analyzed by nano-liquid chromatography followed by direct peptide mass identification (Table 3). This analysis confirmed that both RbsB-His_6 and TNT.R3-His_6 are produced by *E. coli* BW25113 Δ*rbsB* from the P_{AA}-promoter. However, whereas we identified RbsB-His_6 in the whole soluble and in the periplasmic

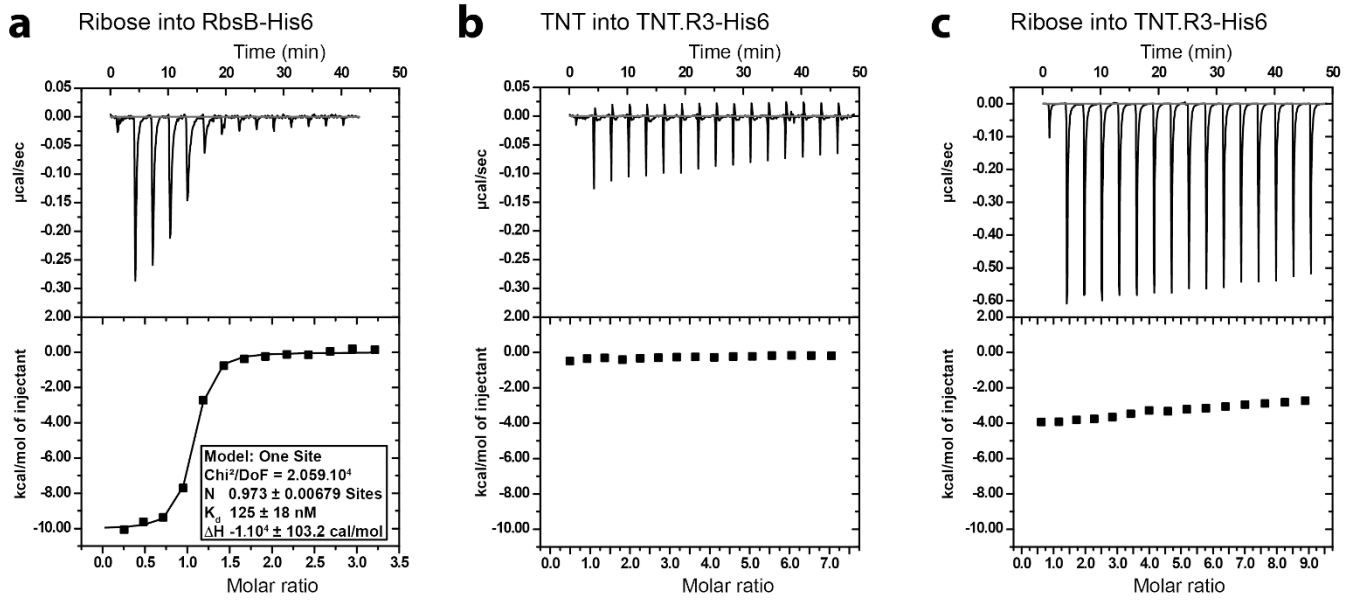

Figure 3 | ***In vitro*** **substrate binding using isothermal microcalorimetry.** (a) Injections of 250 nM ribose into 34 μM purified RbsB-His_6 solution. (b) Injections of 1 μM TNT into 50 μM purified TNT.R3-His_6 solution. (c) Injections of 1 μM ribose into 50 μM purified TNT.R3-His_6 solution. Graphs display immediate heat release in μcal/s (upper panels) and calculated heat release per mol of injectant (lower panels). Note the expected binding of ribose to RbsB (A), but the absence of any detectable binding of TNT or ribose by TNT.R3. For further controls see SI Figure 1.

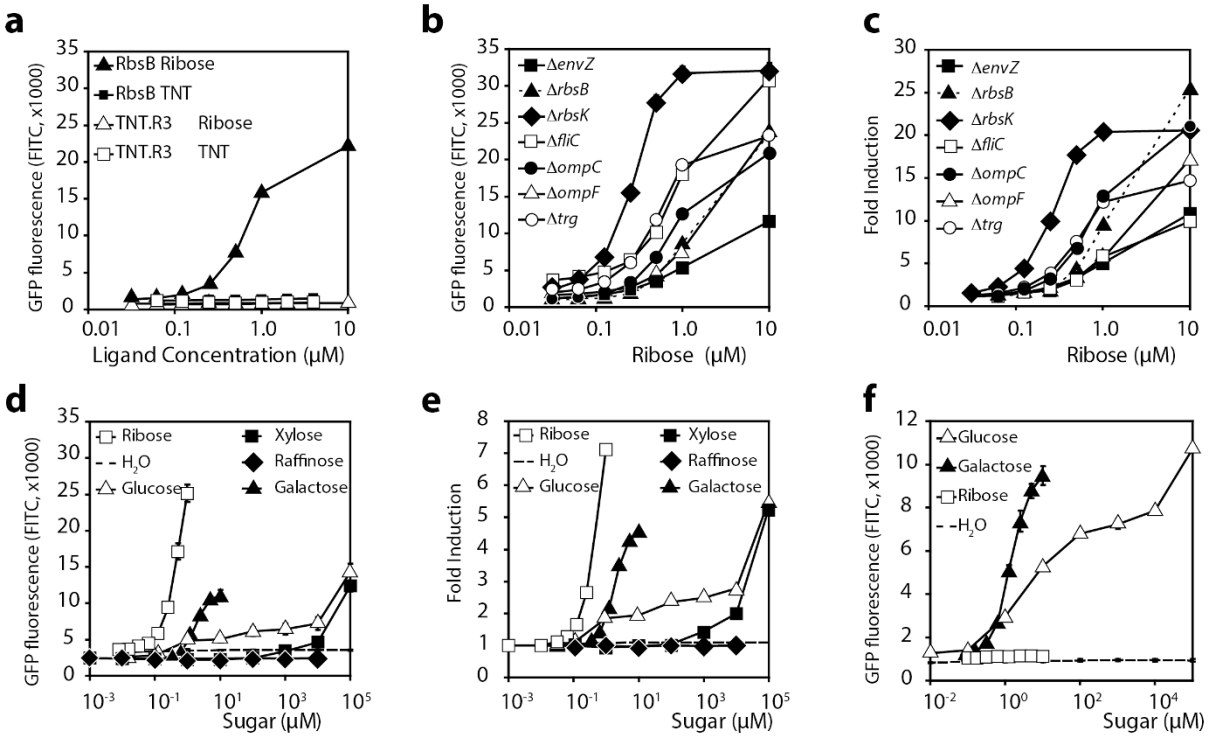

Figure 4 | Reporter gene expression from the hybrid TrzI-OmpR-*ompCp::gfpmut2* signaling chain. (a) Average GFPmut2 fluorescence in flow cytometry (detected using the FITC channel, arbitrary units), as a function of ribose or TNT concentration after 2 h induction time, for *E. coli* BW25113 *ΔrbsB* expressing *rbsB-his6* (strain 4175) or *tnt.r3-his6* (strain 4176). (b) As A, but as a function of ribose exposure only and for a range of *E. coli* BW25113 backgrounds (Table 2). (c) As B, but expressed as -fold induction compared to the blank. (d) As A, but as a function of exposure to different sugars for *E. coli* BW25113 *ΔrbsB* expressing *rbsB-his6* (strain 4175). (e) As D, but expressed as -fold induction compared to the blank. (f) Average GFPmut2 fluorescence of *E. coli* BW25113 *ΔrbsB* (pSYK1, pSTV28, strain 4497) exposed to glucose, galactose or ribose. Data points show means of GFPmut2 fluorescence from biological triplicate assays, each sampling 10,000 cells. Error bars indicate calculated standard deviations from the mean (when not visible, inside symbol size).

protein extracts, TNT.R3-His_6 was only detectable in the whole soluble but not in the periplasmic protein extract (Table 3). We conclude from this part that whereas both RbsB-His_6 and TNT.R3-His_6 are produced from the same plasmid type and promoter in *E. coli*, TNT.R3-His_6 is less abundant and does not seem to be transported into the periplasmic space.

Discussion

We revisit here the use of a PBP-based microbial biosensor, proposed over a decade ago as a general scaffold for computational design of new binding specificities[8,30]. We show through independent *de novo* synthesis that a wild-type RbsB-based signaling cascade is fully functional in detecting low concentrations of ribose, but one of the most interesting computationally designed variants for detecting TNT[8] is not. We conclude this from three different experimental lines of evidence. First, we demonstrated that the purified RbsB bound ribose, as expected, whereas purified TNT.R3 protein bound neither TNT nor ribose at detectable levels (Fig. 3). Second, constitutive expression of *rbsB-his6* under a moderate promoter in an *E. coli* harboring the TrzI hybrid receptor and *ompCp-gfpmut2* fusion led to a ribose-dependent production of GFPmut2 fluorescence already at 50 nM ribose (Fig. 4a, c). In contrast, assays in the same genetic background and plasmid constructions with a *tnt.R3-his6* gene produced no detectable GFPmut2 in presence of either TNT or ribose (Fig. 4a). Finally, we showed that both RbsB-His_6 and TNT.R3-His_6 are produced in such *E. coli* background, but whereas RbsB-His_6 appears to reach the periplasmic space we did not find evidence that this is also true for TNT.R3-His_6 (Fig. 2c, Table 3). The absence of any reporter signal in strains carrying the *tnt.r3-his6* gene to TNT is, therefore, unlikely the result of poor expression of TNT.R3-His_6. Possibly, the introduced mutations in the TNT.R3 variant that were predicted to turn RbsB into a TNT-binder, made the protein less stable in the cytoplasmic environment (Table 3), and hindered the folding and transport process. In addition, it is possible that the intramolecular movement upon ligand binding, or even the binding to the TrzI receptor, are affected. But since we have no evidence that TNT.R3-His_6 reaches the periplasmic space (Table 3), this is a less likely explanation for the absence of GFPmut2 fluorescence in *tnt.R3-his6* reporter strains. Misfolding of the protein was not specifically examined in our assays, but had been suggested as a reason for concern in other studies performed in order to structurally characterize the computational designs of the receptors[31–33].

We acknowledge that the original study designed a number of periplasmic-binding-protein variants, of which we independently reconstructed only the one proposed as the most prominent[8]. We find that the published TNT.R3 mutant cannot be used as a sensor for the detection of TNT, contrary to the reported lowest detection limit of between 10^{-4} and 10^{-3} μM and a K_d of 2 nM[8], a value 65 times lower than the affinity we measured for the wild type RbsB protein towards ribose (125 nM). These findings, however, do not null the notion that a platform using biosensors based on periplasmic binding proteins could be a powerful tool. Indeed, *E. coli* expressing RbsB in combination with the TrzI-hybrid-OmpR *ompCp-gfpmut2* signaling chain turned out to be an excellent reporter for ribose (method detection limit of ~50 nM), with a good selectivity (no reaction to multiple sugars and 10-fold lower detection threshold of ribose than galactose, Fig. 4). We showed that the response from the hybrid signaling chain could even be further optimized by using an *rbsK*-mutant of *E. coli* rather than *rbsB* (Fig. 4C, D). The higher response of this strain to ribose may be explained by the fact that deleting *rbsK*

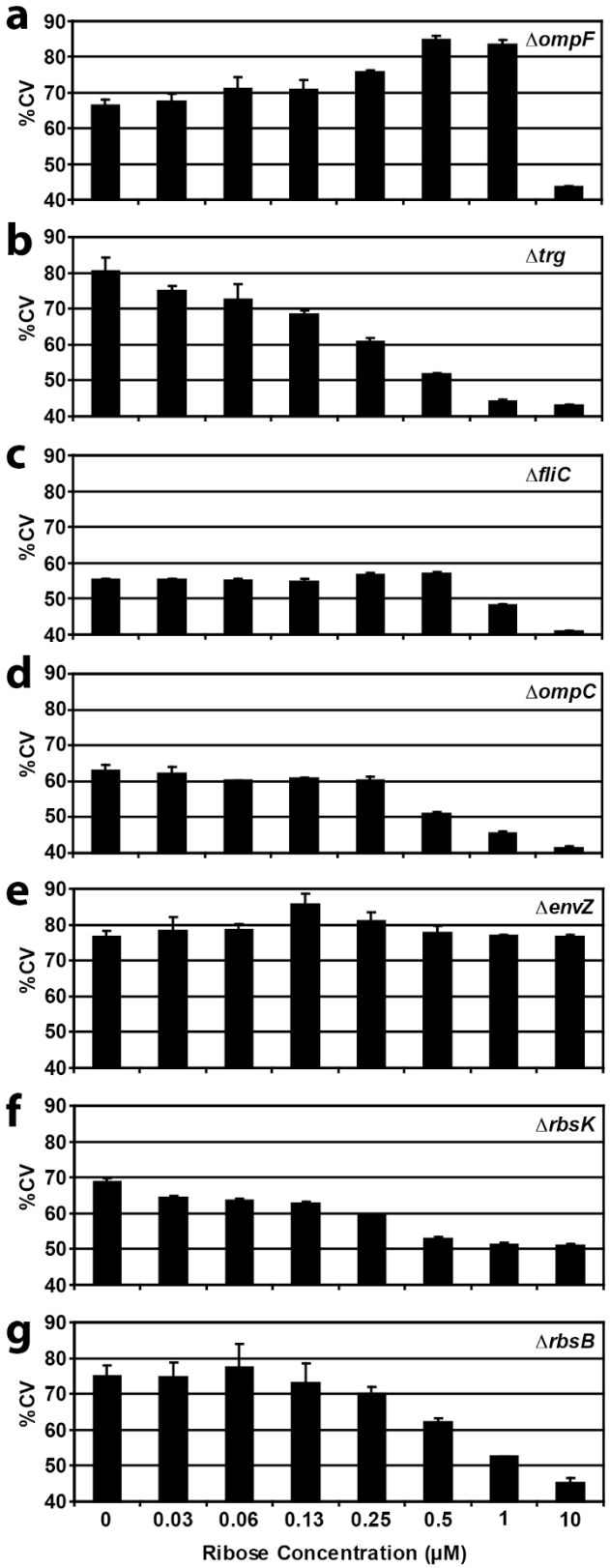

Figure 5 | Coefficient of variation of per-cell GFPmut2 expression as a function of ribose concentration for different *E. coli* BW25113 backgrounds (A–G, Table 2) expressing *rbsB-his6* from pAR3 and the TrzI-OmpR-*ompCp::gfpmut2* hybrid signaling chain of pSYK1. Bars indicate the mean coefficient of variation from biological triplicate assays (each measuring GFPmut2 expression in 10,000 cells), plus one calculated standard deviation (error bar).

interrupts ribose metabolism, leaving on average more ribose to activate the signaling chain through RbsB-TrzI-OmpR rather than going through the ribose transport system. Also, a *trg* host mutant background produced a more sensitive response, but with overall lower fold-induction (Fig. 4c), which may be due to less internal competition for ribose-bound RbsB by the natural Trg chemotaxis receptor. Deletion of *envZ, ompF*, and, surprisingly, *fliC*, resulted in a much poorer response to ribose (Fig. 4b, c). Disruption of native *envZ* may result, in spite of the presence of TrzI, in a lower overall amount of OmpR ~ P in the cell, causing less frequent binding to the weak-affinity OmpR-sites in the P_{ompC} promoter, and thus to a lower level of *gfpmut2* transcription. These results show that the host chassis for a ribose-binding protein based reporter may be further improved and would prove useful, once the limitations in computational design are overcome.

Along with techniques such as directed evolution, computational protein design has been successful in the design of enzyme catalysts, new protein folds, or antigens, but its predictions still fall short especially in the protein-small molecule domain[34–36]. Many methods adopted in the current context, including the technique of dead-end elimination along with a semi-empirical potential energy function, used in designing TNT.R3 and other PBP-variant receptors[8], do not take into consideration the flexibility of the protein backbone. This concerns specifically the substrate binding pocket flexibility, dynamics of the structure upon binding, and calculation of the protein stability or consistency of the 3D fold of the designs. Because of the magnitude of the combinatorial search problem to be tackled in protein design, the chemical accuracy of the calculations is significantly reduced. For a receptor like RBP, the energetic or entropic cost of the conformational re-organization or domain re-orientation during binding can be very important but difficult to calculate. This also holds for other relevant steps in the PBP signalling cascade, such as the binding of the ligand-bound PBP with the transmembrane receptor. So far, therefore, these steps have not been included in energy calculations.

Very recently, it has been demonstrated that *in-silico* design of small-molecule binding proteins can drive the binding affinity down to picomolar level[37]. The computational method was modified so that the designs have binding pockets similar to the naturally occurring ones, in terms of the favourable hydrogen-bonding or van der Waals interactions with the ligand, and high shape complementarity to the ligand. These advances may be highly beneficial for the design of sensory proteins and extremely advantageous to the biosensing field, given that the set of known characterized transcription factors is small and in view of the difficulties involved in the identification of suitable transcription factors for the detection of new compounds of interest.

Methods

Strains and growth conditions. All *E. coli* strains used for this work are listed in Table 2. For cloning purposes, *E. coli* strains were cultured at 37°C on Luria Bertani (LB) medium[38], supplemented with appropriate antibiotics to select for plasmid maintenance. In case of ampicillin (Amp), a concentration of 100 μg/ml was used; for chloramphenicol (Cm), we used 30 μg/ml. Culturing conditions for protein overexpression and for reporter assays are specified below.

Plasmid constructions. The mutant *tnt.R3* gene was produced by DNA synthesis (DNA2.0, CA, USA) on the basis of the mutant sequence provided in Looger *et al*[8]. The gene sequence further encoded a C-terminal hexahistidine (His_6) tag, restriction sites for NdeI (N-terminal), XhoI and BamHI (C-terminal), and for NcoI at the end of the signal sequence (Figure S2). The wild type *rbsB* gene was amplified from pAI12 (a kind gift of Hazelbauer's lab, Pullman, Washington) using primers with restriction sites for NdeI and XhoI. The PCR product was digested and placed into pET22b(+) in order to attach the vector-located hexahistidine tag to the C-terminus of the *rbsB* gene. The resulting *rbsB-*His_6 gene was again amplified with primers containing NdeI and SalI restriction sites. The P_{AA} promoter[29] used to drive constitutive transcription of both *tnt.R3* and *rbsB* was synthesized (DNA2.0) under inclusion of BamHI and SacI restriction sites. The promoter fragment was first cloned into pUC18 and recovered by SacI and XbaI digestion. This P_{AA}-fragment was ligated with a recovered DNA fragment containing the multiple cloning site of pET22(+) (using XbaI and

Table 2 | List of strains used in this study with their relevant characteristics

Strain No	Host	Plasmid(s)	Relevant characteristics	Reference
97	*E. coli* BL21 (DE3)	pLysS	Host strain for overexpression from the T7 promoter	[40]
3325	*E. coli* BL21 (DE3) pLysS	pAR2	Host 97, cytoplasmic overexpression of His6-tagged TNT.R3	This study
3725	*E. coli* BL21 (DE3) pLysS	pAR1	Host 97, cytoplasmic overexpression of His6-tagged RbsB	This study
4076	*Escherichia coli* BW25113 Δ*rbsB*		*rbsB*	[42]
4175	*E. coli* BW25113 Δ*rbsB*	pAR3 pSYK1	expression of His6-tagged RbsB with signal sequence from P_{AA} expression of TrzI, *gfpmut2* fusion to *ompC* promoter	This study
4176	*E. coli* BW25113 Δ*rbsB*	pAR4, pSYK1	as 4175, but expressing the TNT.R3 mutant protein	This study
4497	*E. coli* BW25113 Δ*rbsB*	pSTV28, pSYK1	as 4175, but with empty vector.	This study
4500	*E. coli* BW25113 Δ*ompF*		*ompF*	[42]
4501	*E. coli* BW25113 Δ*trg*		*trg*	[42]
4502	*E. coli* BW25113 Δ*fliC*		*fliC*	[42]
4503	*E. coli* BW25113 Δ*ompC*		*ompC*	[42]
4504	*E. coli* BW25113 Δ*envZ*		*envZ*	[42]
4505	*E. coli* BW25113 Δ*rbsK*		*rbsK*	[42]
4515	*E. coli* BW25113 Δ*ompF*	pAR3, pSYK1	as 4175 in host 4500	This study
4516	*E. coli* BW25113 Δ*trg*	pAR3, pSYK1	as 4175 in host 4501	This study
4517	*E. coli* BW25113 Δ*fliC*	pAR3, pSYK1	as 4175 in host 4502	This study
4518	*E. coli* BW25113 Δ*ompC*	pAR3, pSYK1	as 4175 in host 4503	This study
4519	*E. coli* BW25113 Δ*envZ*	pAR3, pSYK1	as 4175 in host 4504	This study
4520	*E. coli* BW25113 Δ*rbsK*	pAR3, pSYK1	as 4175 in host 4505	This study

SalI), and with pSTV28 (Takara, Japan), digested with SacI and SalI. After transformation in *E. coli*, this resulted in plasmid pSTV28P_{AA}mcs. Finally, *rbsB-His*$_6$ and *tnt.R3-His*$_6$ were placed into pSTV28P_{AA}mcs using NdeI and SalI or NdeI and XhoI, respectively, resulting in pAR3 and pAR4 (Fig. 1b, Table 2).

For overexpression the synthesized *tnt.R3-His*$_6$ fragment was digested with NcoI and BamHI and placed into pET3d[39] resulting in pAR2. This removes the signal sequence for transport in the periplasmic space. *RbsB-His*$_6$ was amplified from pAI12, now without the signal sequence using primers containing NdeI and XhoI restriction sites. The NdeI-XhoI fragment was purified and placed into pET22b(+) digested with the same enzymes, directly in front of the hexahistidine tag. After transformation this resulted in plasmid pAR1. All final constructs were verified by sequencing. Plasmids for overexpression were transformed into *E. coli* BL21 (DE3) carrying pLysS[40].

Plasmid pSYK1 carries the gene for the hybrid receptor *trzI* under the control of P_{tac} and *gfpmut2* under the control of P_{ompC} (Fig. 1b). The *ompC* promoter fused to the *gfpmut2* reporter gene was amplified from plasmid pUA66-ompC::GFPmut2[41] (kindly provided by Prof. Uri Alon from the Department of Molecular Cell Biology at the Weizmann Institute of Science, Rehovot, Israel) using primers that introduced BamHI restriction sites on either end. This fragment was ligated into the unique BamHI site of plasmid pRB020, which carries a *lacIq* gene and places *trzI* under control of the *tac* promoter[24]. After transformation this resulted in plasmid pSYK1. Reporter constructs were cotransformed into *E. coli* BW25113 background carrying either *rbsB* deletion or deletions in other genes of the hybrid signaling pathway (Table 2).

Analysis of expression of RbsB-His$_6$ and TNT.R3-His$_6$ in *E. coli* BW25113. Ten mL LB medium containing Amp and Cm were inoculated with a single colony from a freshly grown LB agar plate with both antibiotics, and incubated at 37°C. The cells were harvested by centrifugation at 3200 x g at mid-exponential phase (OD_{600} = 0.7) and resuspended in 400 µL of 30 mM Tris-HCl containing 20% sucrose at a pH of 8.0. Half of the suspension (for the preparation of the total soluble protein fraction or cell extract) was transferred to 1.5 mL screw-capped microtubes containing 0.1 g acid-washed glass beads (<106 µm, Sigma, USA). Suspensions were homogenized in a bead beater (Fastprep FP120, Thermo Electron, USA) for 30 s at a speed of 4.0. EDTA was added to the other half to a final concentration of 1 mM for the preparation of the soluble periplasmic protein fraction. This suspension was incubated on ice for 10 min with gentle agitation. After centrifugation at 16,000 x *g* for 20 min at 4°C the supernatant was removed and the pellet was resuspended in 200 µL of ice-cold solution of 5 mM $MgSO_4$. During the following incubation on ice for 10 min the tubes were inverted 10 times every minute for 10 s. Both whole soluble and periplasmic fractions were centrifuged for 30 min at 16,000 x *g* and 4°C, after which the supernatant was transferred to a clean Eppendorf tube and placed on ice. Samples were then analyzed by SDS-polyacrylamide gel electrophoresis (PAGE), by mixing various protein amounts with SDS loading buffer, according to Sambrook[38]. Samples for SDS-PAGE were incubated for 5 min on a thermomixer (Eppendorf, Schweiz) at 99°C, and centrifuged for 1 min at 16,000 x *g* immediately before loading. The samples were loaded onto 13% acrylamide gel and proteins were separated for 1.5 h at 150 V, according to standard procedures[38].

After electrophoresis the gels were stained using InVision colorant (Life technologies, USA) in order to detect His_6-tagged proteins. The gel was placed into a fixing solution (40% v/v ethanol and 10% v/v acetic acid in ultrapure water) for 1 h and then washed with water for 20 min. Subsequently, the gel was washed with buffer A (20 mM imidazole, 50 mM NaH_2PO_4 and 500 mM NaCl, pH 8.0) for 10 min, and incubated with InVision stain for 1 h. The gel was destained with 20 mM phosphate buffer (pH 7.8) for 20 min, and subsequently scanned on a Typhoon imager (Amersham Biosciences, United Kingdom) at a resolution of 50 µm using a 532 nm laser. Subsequently, gels were washed with water for 10 min, and restained using Coomassie blue for 1 h according to standard procedures[38]. After destaining the gel was photographed with a Nikon D5100 camera equipped with a 18–55 mm objective (Nikon, Schweiz) under white light illumination.

Table 3 | Occurrence of RbsB-His$_6$ and TNT.R3-His$_6$ in *E. coli* BW25113 Δ*rbsB* (pSYK1) protein fractions

	Periplasmic protein fraction[1]			Whole soluble protein fraction[1]		
Identified protein(s)	Strain 4175 RbsB-His$_6$	Strain 4176 TNT.R3-His$_6$	Strain 4497 Ctrl	Strain 4175 RbsB-His$_6$	Strain 4176 TNT.R3-His$_6$	Strain 4497 Ctrl
RbsB-His$_6$	18 (8)[2]	5 (5)	4 (4)	14 (5)	1 (1)	1 (1)
TNT.R3-His$_6$	ND[3]	ND	ND	ND	2 (2)	ND
RbsB-His$_6$ + TNT.R3-His$_6$[4]	18 (5)	6 (6)	ND	10 (5)	5 (3)	ND
Total RbsB-His$_6$ + TNT.R3-His$_6$[5]	36 (13)	11 (11)	4 (4)	24 (10)	8 (6)	1 (1)
Total proteins	116 (387)[6]	86 (277)[6]	104 (349)[6]	259 (1273)[6]	234 (971)[6]	254 (1061)[6]

1) 28–36 kD fragments on SDS-PAGE gel from extracts as shown in Fig. 2C, originating from *E. coli* BW25113 Δ*rbsB* (pSYK1) expressing *rbsB-his6* (from plasmid pAR3, strain 4175), *E. coli* BW25113 Δ*rbsB* (pSYK1) expressing *tnt.R3-his6* (from plasmid pAR4, strain 4176), or *E. coli* BW25113 Δ*rbsB* (pSYK1) carrying empty pSTV (strain 4497, Ctrl).
2) Normalized number of peptide mass fragments identifying the protein(s) as total number of specific peptide fragments by the averaged total peptide count in the sample; between brackets, number of unique peptide mass fragments identifying the protein(s).
3) ND, not detected.
4) Peptides covering regions common to both RbsB-His$_6$ and TNT.R3-His$_6$.
5) All peptides identifying both RbsB-His$_6$ and TNT.R3-His$_6$.
6) Total number of identified proteins within the 27–32 kDa purified gel region; within brackets: total number of identified peptide mass fragments.

Expression and export of RbsB-His_6 and TNT.R3-His_6 from the P_{AA}-promoter was separately analyzed using direct peptide mass identification. *E. coli* BW25113 cultures were grown and periplasmic or whole soluble protein fractions were prepared as described above. Proteins were separated by SDS-PAGE and proteins in a size region of 28-36 kD were excised. Proteins were subsequently digested with trypsin and peptides were separated on an Ultimate 3000 Nano LC System (Dionex), followed by detection in a Thermo Scientific LTQ-Orbitrap XL mass spectrometer (Thermo Fisher Scientific, Waltham, MA). Mass spectra were analyzed using Scaffold Viewer (http://www.proteomesoftware.com/), using protein and peptide identification thresholds of 99.9% and 99.99%, respectively. The minimum number of peptides for identification was 2.

RbsB-His_6 and TNT.R3-His_6 overexpression and purification. In order to analyze *in vitro* substrate binding, we first overexpressed and purified RbsB-His_6 and TNT.R3-His_6. We used the C-terminal added hexahistidine tag in combination with Ni-NTA affinity column chromatography (Qiagen, Germany). Proteins were overexpressed in *E. coli* BL21(DE3)pLysS carrying the appropriate plasmid (pAR1 for RbsB-His_6 or pAR2 for TNT.R3-His_6). Cultures were launched at 37°C in 200 mL LB medium containing 100 μg/mL Amp and 30 μg/mL Cm and inoculated with a single colony from a freshly grown agar plate. At a culture turbidity of $OD_{600} = 0.3$ overexpression was induced through addition of IPTG to 1 mM final concentration. Cultures were incubated further for 16 h at 20°C, after which the cells were harvested by centrifugation at 3,200 x g in four 50 mL Falcon tubes. Cell pellets were stored at −80°C until protein isolation.

For purification of the His_6-tagged proteins, one cell pellet was resuspended in 4 mL of buffer A (see above). The suspension was transferred into 1.5 mL screw-capped plastic tubes containing 0.1 g glass beads (see above), and homogenized in a bead beater (Fastprep) for 3 times at 20 s and a speed of 4.0, with intermittent cooling on ice. After centrifugation for 30 min at 16,000 x *g* and 4°C the supernatant was transferred to a clean tube, and mixed with 750 μL of Ni-NTA resin (Qiagen, Germany) for one hour at 4°C using a multi axle rotator (A257, Denley Instruments LTD, United Kingdom). Subsequently, the protein-Ni-NTA suspension was poured onto a 1 mL polypropylene column (Qiagen, Germany) to collect the protein-bound-resin. After consecutive washing with 1 mL of buffer A containing first 40 mM and then 80 mM imidazole, the proteins were eluted in fractions of 600 μL using buffer A containing 250 mM imidazole. Flow-through from the column was collected and analysed by SDS-PAGE and Coomassie blue staining (see above). Protein concentrations were determined by using the Bradford assay and by NanoDrop spectrophotometry (Thermo Scientific, USA), using the "Protein A280" mode with calculated theoretical molar extinction coefficient and molecular weight as parameters. Purified protein was stored on ice and used within 5 h for the substrate-binding assay, without further dialysis.

Analysis of substrate binding using isothermal microcalorimetry (ITC). Quantified amounts of purified protein, typically 280 μl of between 0.6 and 1 μg/μl, were pipetted into the measurement cell of an isothermal titration calorimetry instrument (MicroCal iTC200, GE Healthcare Life Sciences, USA). A volume of 280 μl of elution buffer (buffer A with 250 mM imidazole) was used as a reference. An appropriate concentration of the test ligand (of between 0.25 and 1 mM in buffer A containing 250 mM imidazole) was filled into the injection syringe. In other experiments we tested injecting purified protein solution (of between 1.4 and 2.8 μg/μl) into substrate solution in the measurement cell. The substrates tested were ribose and TNT. Measurements were taken at 20°C, with a reference power of 11 μcal/s, a stirring velocity of 1000 rpm and a "low feedback" mode. Raw data were recorded in μcal/s over time and integrated to kcal/mol over molar ratio. Wherever possible regression curves were calculated based on a one-binding site model.

RBP-based bioreporter assays using the TrzI-OmpR hybrid signaling chain. In order to measure the capacity of RbsB or TNT.R3 to induce the TrzI-hybrid-OmpR *ompCp-gfpmut2* signaling chain in the presence of appropriate inducer, we used *E. coli* BW25113Δ*rbsB* cotransformed with pSTV-based plasmids (pAR3, to express *rbsB*, or pAR4 for *tnt.R3*) and plasmid pSYK1 (to provide the hybrid signaling chain, see Table 2). Upon induction, these strains produce GFPmut2, the fluorescence intensity of which was measured using flow cytometry. The bioreporter assay was optimized for minimal background GFPmut2 expression and medium fluorescence. Hereto, 5 mL of minimal medium with Amp and Cm (SI Table 1) with 20 mM fumarate as sole carbon and energy source were inoculated with a single colony from a freshly grown LB plate containing the same antibiotics. Cultures were incubated overnight at 37°C with rotary shaking at 180 rpm. The next morning, 2 μL culture aliquots were transferred into 5 mL of fresh minimal medium (SI Table 1), and incubated for 4 h at 37°C with rotary shaking at 180 rpm. Samples (180 μL) of this culture were then introduced into the wells of a 96-well plate (F96 Cert.Maxisorp, Nunc, Denmark) and mixed with 20 μL of the appropriate ligand in a range of concentrations to start induction. Notably, we used ribose (D-(-)-ribose, Aldrich, USA) at concentrations between 7.8 nM and 250 μM. 2,4,6-Trinitrotoluene (TNT) was purchased from Dr. Ehrenstorfer GmbH, Germany and used at concentrations between 62 nM and 4 μM, by dissolving the TNT in water. Different other gene deletion variants of BW25113[42] were tested with the same plasmids, in order to discern the effect of background host genes on the induction from the hybrid signalling chain (Table 2). Induction was allowed to proceed for 2 h at 37°C, after which aliquots of 150 μl of each of the wells were auto-sampled, and values of individual cell forward scatter (FSC) and GFPmut2 fluorescence (FITC-channel) were recorded by a Becton Dickinson Fortessa flow cytometer (LRS FortessaTM, Becton Dickinson, USA). The flow rate was set to 3 μl/s and the cell density was between 100-1000 cells/μL. Sensitivities for the FSC and the FITC channels were set at 350 V and 676 V, respectively. Recorded data were gated to remove background particles. The mean fluorescence values of the gated uninduced or induced populations were calculated. All experiments were carried out in triplicate, and the standard deviation and coefficient of variation were calculated from the mean fluorescence.

1. Siegfried, K. *et al.* Field testing of arsenic in groundwater samples of Bangladesh using a test kit based on lyophilized bioreporter bacteria. *Environ Sci Technol* **46**, 3281–3287 (2012).
2. Pedahzur, R., Polyak, B., Marks, R. S. & Belkin, S. Water toxicity detection by a panel of stress-responsive luminescent bacteria. *J Appl Toxicol* **24**, 343–348 (2004).
3. Branco, R., Cristovao, A. & Morais, P. V. Highly sensitive, highly specific whole-cell bioreporters for the detection of chromate in environmental samples. *PLoS One* **8**, e54005 (2013).
4. Farhan Ul Haque, M., Nadalig, T., Bringel, F., Schaller, H. & Vuilleumier, S. Fluorescence-based bacterial bioreporter for specific detection of methyl halide emissions in the environment. *Appl Environ Microbiol* **79**, 6561–6567 (2013).
5. Munoz-Martin, M. A., Mateo, P., Leganes, F. & Fernandez-Pinas, F. A battery of bioreporters of nitrogen bioavailability in aquatic ecosystems based on cyanobacteria. *Sci Total Environ* **47**, 2050–2064 (2013).
6. Stocker, J. *et al.* Development of a set of simple bacterial biosensors for quantitative and rapid field measurements of arsenite and arsenate in potable water. *Environ Sci Technol* **37**, 4743–4750 (2003).
7. van der Meer, J. R. & Belkin, S. Where microbiology meets microengineering: design and applications of reporter bacteria. *Nat Rev Microbiol* **8**, 511–522 (2010).
8. Looger, L. L., Dwyer, M. A., Smith, J. J. & Hellinga, H. W. Computational design of receptor and sensor proteins with novel functions. *Nature* **423**, 185–189 (2003).
9. Merulla, D. *et al.* Bioreporters and biosensors for arsenic detection. Biotechnological solutions for a world-wide pollution problem. *Curr Opin Biotechnol* **24**, 534–541 (2013).
10. Hynninen, A. & Virta, M. Whole-cell bioreporters for the detection of bioavailable metals. *Adv Biochem Eng Biotechnol* **118**, 31–63 (2010).
11. Ivask, A., Rolova, T. & Kahru, A. A suite of recombinant luminescent bacterial strains for the quantification of bioavailable heavy metals and toxicity testing. *BMC Biotechnol* **9**, 41 (2009).
12. Sticher, P., Jaspers, M., Harms, H., Zehnder, A. J. B. & van der Meer, J. R. Development and characterization of a whole cell bioluminescent sensor for bioavailable middle-chain alkanes in contaminated groundwater samples. *Appl Environ Microbiol* **63**, 4053–4060 (1997).
13. Belkin, S. A panel of stress-responsive luminous bacteria for monitoring wastewater toxicity. *Methods Mol Biol* **102**, 247–258 (1998).
14. de las Heras, A. & de Lorenzo, V. In situ detection of aromatic compounds with biosensor *Pseudomonas putida* cells preserved and delivered to soil in water-soluble gelatin capsules. *Anal Bioanal Chem* **400**, 1093–1104 (2011).
15. Galvao, T. C. & de Lorenzo, V. Transcriptional regulators a la carte: engineering new effector specificities in bacterial regulatory proteins. *Curr Opin Biotechnol* **17**, 34–42 (2006).
16. Garmendia, J., Devos, D., Valencia, A. & de Lorenzo, V. A la carte transcriptional regulators: unlocking responses of the prokaryotic enhancer-binding protein XylR to non-natural effectors. *Mol Microbiol* **42**, 47–59 (2001).
17. Reed, B., Blazeck, J. & Alper, H. Evolution of an alkane-inducible biosensor for increased responsiveness to short-chain alkanes. *J Biotechnol* **158**, 75–79 (2012).
18. Beggah, S., Vogne, C., Zenaro, E. & van der Meer, J. R. Mutant transcription activator isolation via green fluorescent protein based flow cytometry and cell sorting. *Microb Biotechnol* **1**, 68–78 (2008).
19. Grimm, S., Salahshour, S. & Nygren, P. A. Monitored whole gene in vitro evolution of an anti-hRaf-1 affibody molecule towards increased binding affinity. *Nat Biotechnol* **29**, 534–542 (2012).
20. Mustafi, N., Grunberger, A., Kohlheyer, D., Bott, M. & Frunzke, J. The development and application of a single-cell biosensor for the detection of l-methionine and branched-chain amino acids. *Metab Eng* **14**, 449–457 (2012).
21. Chu, B. C. & Vogel, H. J. A structural and functional analysis of type III periplasmic and substrate binding proteins: their role in bacterial siderophore and heme transport. *Biol Chem* **392**, 39–52 (2011).
22. Binnie, R. A., Zhang, H., Mowbray, S. & Hermodson, M. A. Functional mapping of the surface of *Escherichia coli* ribose-binding protein: mutations that affect chemotaxis and transport. *Protein Sci* **1**, 1642–1651 (1992).
23. Riley, M. Functions of the gene products of *Escherichia coli*. *Microbiol Rev* **57**, 862–952 (1993).
24. Baumgartner, J. W. *et al.* Transmembrane signalling by a hybrid protein: communication from the domain of chemoreceptor Trg that recognizes sugar-binding proteins to the kinase/phosphatase domain of osmosensor EnvZ. *J Bacteriol* **176**, 1157–1163 (1994).
25. Inouye, M. Signaling by transmembrane proteins shifts gears. *Cell* **126**, 829–831 (2006).
26. Srividhya, K. V. & Krishnaswamy, S. A simulation model of *Escherichia coli* osmoregulatory switch using E-CELL system. *BMC Microbiol* **4**, 44 (2004).

27. Dwyer, M. A. & Hellinga, H. W. Periplasmic binding proteins: a versatile superfamily for protein engineering. *Curr Opin Struct Biol* **14**, 495–504 (2004).
28. Breijo, E. G. *et al.* TNT detection using a voltammetric electronic tongue based on neural networks. *Sensors and Actuators A: Physical* **192**, 1–8 (2013).
29. Alper, H., Fischer, C., Nevoigt, E. & Stephanopoulos, G. Tuning genetic control through promoter engineering. *Proc Natl Acad Sci USA* **102**, 12678–12683 (2005).
30. Dwyer, M. A., Looger, L. L. & Hellinga, H. W. Computational design of a Zn2+ receptor that controls bacterial gene expression. *Proc Natl Acad Sci U S A* **100**, 11255–11260 (2003).
31. Schreier, B., Stumpp, C., Wiesner, S. & Hocker, B. Computational design of ligand binding is not a solved problem. *Proc Natl Acad Sci U S A* **106**, 18491–18496 (2009).
32. Antunes, M. S. *et al.* Programmable ligand detection system in plants through a synthetic signal transduction pathway. *PLoS One* **6**, e16292 (2011).
33. Service, R. F. Protein designers go small. *Science* **341**, 1052 (2013).
34. Boas, F. E. & Harbury, P. B. Design of protein-ligand binding based on the molecular- mechanics energy model. *J Mol Biol* **380**, 415–424 (2008).
35. Azoitei, M. L. *et al.* Computation-guided backbone grafting of a discontinuous motif onto a protein scaffold. *Science* **334**, 373–376 (2011).
36. Kiss, G., Çelebi-Ölçüm, N., Moretti, R., Baker, D. & Houk, K. N. Computational enzyme design. *Angew Chem Int Ed Engl* **52**, 5700–5725 (2013).
37. Tinberg, C. E. *et al.* Computational design of ligand-binding proteins with high affinity and selectivity. *Nature* **501**, 212–216 (2013).
38. Sambrook, J. & Russell, D. W. *Molecular cloning: a laboratory manual.* third edn, (Cold Spring Harbor Laboratory Press, 2001).
39. Rosenberg, A. H. *et al.* Vectors for selective expression of cloned DNAs by T7 RNA polymerase. *Gene* **56**, 125–135 (1987).
40. Studier, F. W. & Moffatt, B. A. Use of bacteriophage T7 RNA polymerase to direct selective high-level expression of cloned genes. *J Mol Biol* **189**, 113–120 (1986).
41. Zaslaver, A. *et al.* A comprehensive library of fluorescent transcriptional reporters for *Escherichia coli*. *Nat Methods* **3**, 623–628 (2006).
42. Baba, T. *et al.* Construction of *Escherichia coli* K-12 in-frame, single-gene knockout mutants: the Keio collection. *Mol Syst Biol* **2**, 2006 0008 (2006).

Acknowledgments

This work was supported by grant 244405 (Biomonar) from the European Seventh Framework Programme (FP7). The pAI12 plasmid was kindly provided by Hazelbauer's lab (Washington State University, USA). We thank Sebastian Ritzmann for help in optimizing RbsB protein purification and Karine Lapouge for instructions in ITC measurements. Patrice Waridel and Manfredo Quadroni from the University of Lausanne Protein Analysis Facility are thanked for their help in peptide analysis. Work in the Belkin lab was partially supported by the Minerva Center for Bio-hybrid Complex Systems.

Author contributions

A.R. and S.Y.K. performed experiments. A.R. and J.R.M. prepared Figures 1–5. S.B. and S.Y.K. contributed strains and experimental advice. A.R., S.R. and J.R.M. wrote the main manuscript. All authors reviewed the final manuscript.

Additional information

Supplementary information accompanies this paper at http://www.nature.com/scientificreports

Competing financial interests: The authors declare no competing financial interests.

How to cite this article: Reimer, A., Yagur-Kroll, S., Belkin, S., Roy, S. & van der Meer, J.R. *Escherichia coli* ribose binding protein based bioreporters revisited. *Sci. Rep.* **4**, 5626; DOI:10.1038/srep05626 (2014).

SCIENTIFIC REPORTS

DOI: 10.1038/srep07445

SUBJECT AREAS:
APPLIED MICROBIOLOGY
ASSAY SYSTEMS

SCIENTIFIC REPORTS:
4 : 5626
DOI: 10.1038/srep05626
(2014)

Published:
9 July 2014

Updated:
19 December 2014

CORRIGENDUM: *Escherichia coli* ribose binding protein based bioreporters revisited

Artur Reimer, Sharon Yagur-Kroll, Shimshon Belkin, Shantanu Roy & Jan Roelof van der Meer

The original version of this Article contained an error in the title of the paper, where the word "*Escherichia*" was incorrectly given as "*Escherchia*". This has now been corrected in both the PDF and HTML versions of the Article.